Video lensfree microscopy of 2D and 3D cultures of cells

C.P. Allier[1], S. Vinjimore Kesavan[1], J.-G. Coutard[1], O. Cioni[1], F. Momey[1], F. Navarro[1], M. Menneteau[1], B. Chalmond[2,3], P. Obeïd[4,5,6], V. Haguet[4,5,6], B. David-Watine[7], N. Dubrulle[7], S. Shorte[7], B. van der Sanden[8], C. Di Natale[8], L. Hamard[8], D. Wion[8], M.E. Dolega[4,5,6], N. Picollet-D'hahan[4,5,6], X. Gidrol[4,5,6], J.-M. Dinten[1]

[1]CEA, Leti, Campus Minatec, Grenoble France, [2]University of Cergy-Pontoise & CMLA, [3]ENS-Cachan, [4]CEA, iRTSV, Laboratoire Biologie à Grande Echelle, Grenoble, France, [5]INSERM, U1038, [6]Université Grenoble-Alpes, France, [7]Institut Pasteur, Paris France, [8]Clinatec, CEA, Campus Minatec, Grenoble France

ABSTRACT

Innovative imaging methods are continuously developed to investigate the function of biological systems at the microscopic scale. As an alternative to advanced cell microscopy techniques, we are developing lensfree video microscopy that opens new ranges of capabilities, in particular at the mesoscopic level. Lensfree video microscopy allows the observation of a cell culture in an incubator over a very large field of view (24 mm^2) for extended periods of time. As a result, a large set of comprehensive data can be gathered with strong statistics, both in space and time. Video lensfree microscopy can capture images of cells cultured in various physical environments. We emphasize on two different case studies: the quantitative analysis of the spontaneous network formation of HUVEC endothelial cells, and by coupling lensfree microscopy with 3D cell culture in the study of epithelial tissue morphogenesis. In summary, we demonstrate that lensfree video microscopy is a powerful tool to conduct cell assays in 2D and 3D culture experiments. The applications are in the realms of fundamental biology, tissue regeneration, drug development and toxicology studies.

Keywords: Lensfree imaging, cell culture, 3D cell culture, video microscopy

1. INTRODUCTION

Our ability to address fundamental issues concerning the evolution and organization of tissues and cell populations has strongly progressed for the last decades through increasingly powerful optical instruments. However, fundamental biology questions remain unanswered at mesoscopic scales [1-4]. We are developing video lensfree microscopy as an alternative method to bring new perspectives for the characterization of biological systems. Our lensfree video microscope aims at:

- Multiscale observation capability across two orders of magnitude, *e.g.*, tissues and cells;
- Large field of view of 25 mm^2 or above;
- Live capture or time-lapse capability over long time periods;
- Simplicity of use, small form factor and low cost.

No microscopy technique fully meets the four mentioned guidelines. Even taken separately, these guidelines strongly redefine bio imaging as we know it today. For instance, a compound microscope is meant to observe a small field of view (<1 mm^2) featuring at best few hundreds of cells within a focal plane. At large magnification, very few cells are visible. To gain additional information, microscopy makes use of multiple refinements such as raster scan, fluorescent labeling, time-lapse, super-resolution, *etc.* But clearly this is at the price of larger complexity and cost. In this paper we demonstrate the capabilities of video lensfree microscopy to fulfill most if not all of the guidelines. Lensfree imaging is based on in-line holography as invented by Gabor in 1948 [5]. A biological object is illuminated by a coherent light; the light diffracted by the micrometric structures of the object interferes with the incident wave. The amplitude of the interference is recorded by a photographic sensor. Albeit the method exists since decades, the recent development of digital sensors, popularized by their use in cameras, helped to realize the full potential of lensfree imaging [6-10]. Here

Imaging, Manipulation, and Analysis of Biomolecules, Cells, and Tissues XII, edited by Daniel L. Farkas, Dan V. Nicolau, Robert C. Leif, Proc. of SPIE Vol. 8947, 89471H
 · doi: 10.1117/12.2038098

we describe a lensfree video microscope that allows observing a culture of cells (up to 10,000 cells) in a very large field of view (24 mm^2) for periods of time extending from days to weeks. At first, the ability of the lensfree video microscope to capture images of cells in culture in various physical environments will be presented. Namely several adherent cell lines, including kidney epithelial cells, noncancerous prostate epithelial cells RWPE-1, prostate carcinoma cells PC3, primary human fibroblasts, endothelial cells HUVEC, were cultured and observed in different labware (35 mm Petri dish, 6-wells microtiter plate, *etc.*) over distinct substrates (polylysin, Matrigel, PNIPAM, inside an extra-cellular matrix, *etc.*). The ability of the technique to observe different cell types and also to differentiate the phenotypes is demonstrated. Further, monitoring of cells also in 3D cell culture is shown. Lensfree video microscopy is a powerful tool to conduct experiments using 2D and 3D assays. Similar works can be found in [11-14].

2. MATERIALS AND METHODS

The video microscopy device is based on lensless imaging as described by Ozcan *et al.* [7-10] which was modified to perform continuous monitoring in an incubator at a controlled temperature of 37 °C with humidity typically >80% (Fig. 1). In a typical experiment, the lensfree video microscope is placed inside the incubator and the culture dish containing the cells is placed on top of the lensfree video microscope. The lensfree video microscope features a 12-bit Aptina MT9P031 CMOS RGB image sensor with a pixel pitch of 2.2 µm and an imaging area of 5.7 x 4.3 mm^2. Illumination is provided by an LED along with a 150 µm pinhole placed at a distance of approximately 5 cm from the cells. The temperature of the image sensor in continuous mode can exceed 45 °C, which is not compatible with viability of human cells, a Peltier element is used to maintain the image sensor at 37 °C.

The lensfree imaging setup does not acquire an image of the cell but a holographic interference pattern formed by the interference of the semi-coherent light scattered by the cell and the light passing directly from the source to the image sensor. The distance between the cells and the image sensor is not critical; for distances in the range of 0.5 mm up to 3 mm the 10-20 µm adherent cells provide holographic patterns with good signal-to-noise ratio. In our experiments, the typical distance between the cells and the image sensor is 1.2 mm.

A reconstruction algorithm is then used to recover the overall shape of every cell and their precise location from the interference holographic patterns (Fig. 2). The holographic reconstruction is based on a phase retrieval algorithm as described in [15, 16]. Adherent cells differ from those objects in the sense that their semi-convex shape likely causes a lensing effect which is not taken into account in the holographic reconstruction scheme. The latter considers Fresnel propagation of light and does not take into account the refraction of light occurring at the liquid-cell membrane interface.

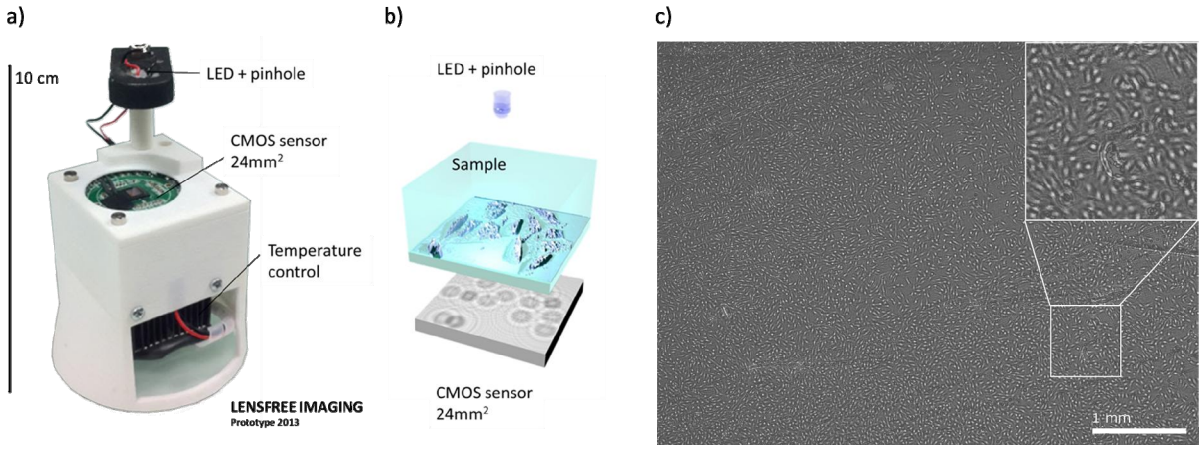

Figure 1. (a) Experimental setup of the Lensfree video microscope. A CMOS image sensor is used for image acquisition and an LED and a 150 µm pinhole for illumination (5 cm above the image sensor). (b) The CMOS image sensor is put in contact with the Petri dish and records the holographic patterns resulting from the interference between the partially coherent incident light and the light scattered by the cells. Lensfree imaging is compatible with an incubation environment and can image 24 mm^2 of, *e.g.*, a standard 35mm Petri dish. (c) The image shows the acquisition of approximately 8,000 fibroblast cells acquired by means of the lensfree video microscope.

3. RESULTS AND DISCUSSION

The reconstruction of the cells obtained from the interference holographic patterns (Fig. 2) is very realistic in comparison with standard observations using optical microscopy. The whole cell population can be monitored and analyzed to provide metrics specific to the cell line and/or applied culture conditions. Possible metrics include the cell number, possible aggregations of cells, cell-cell interactions and duration between successive cell divisions. The trajectories of the cells can be displayed from the set of images acquired in time-lapse mode (Fig. 2b). The reconstructed image provides morphology of the cells with a resolution close to 2 µm (Fig 2c,d). This resolution allows the visualization of single cell motility with filopodial extensions and focal adhesion points (Fig 2c). 3D reconstruction of the cells results from the calculation of phase with a vertical precision of few µm. As an example, Fig. 2d shows, in 3D, a moving cell which later divides (marked by a red arrow). Cell heights of approximately 6-8 µm were calculated, which is coherent with literature.

In summary, the imaging device offers a resolution close to 2 µm over a field of view of 24 mm², which makes it capable of monitoring a cell culture at different scales, from a very large field of view down to the single cell. As a consequence, lensfree imaging can support applications in fundamental biology, tissue regeneration, drug development and toxicology studies in which the number, position and shape of the cells are sufficient information and no intracellular detail of the cells is required. As a drawback, our lensfree video microscope is not able to measure fluorescence which has settle many if not all of recent observation and studies in modern biology can also be mentioned. Recent developments overcome these limitations [11,17,18] but again at the price of complexity which prevents routine experiments in an incubator. Yet one must emphasize that cell imaging is not only about taking pictures with high resolution and labeling with many fluorescent dyes. As important is gathering information from the images images for characterizing important events with relevant statistics. Lensfree microscopy at the mesoscopic level (24 mm^2 field of view) provides statistically relevant data relying on the simultaneous observation of thousands of cells over days to weeks. In the following, we will focus in particular on the mesoscopic level which is critical in cell biology [1-4]. Significant biological processes, *i.e.*, cell population organization and its evolution over time, will be used to demonstrate that high spatial resolution is not necessary to extract important features of the cell cultures.

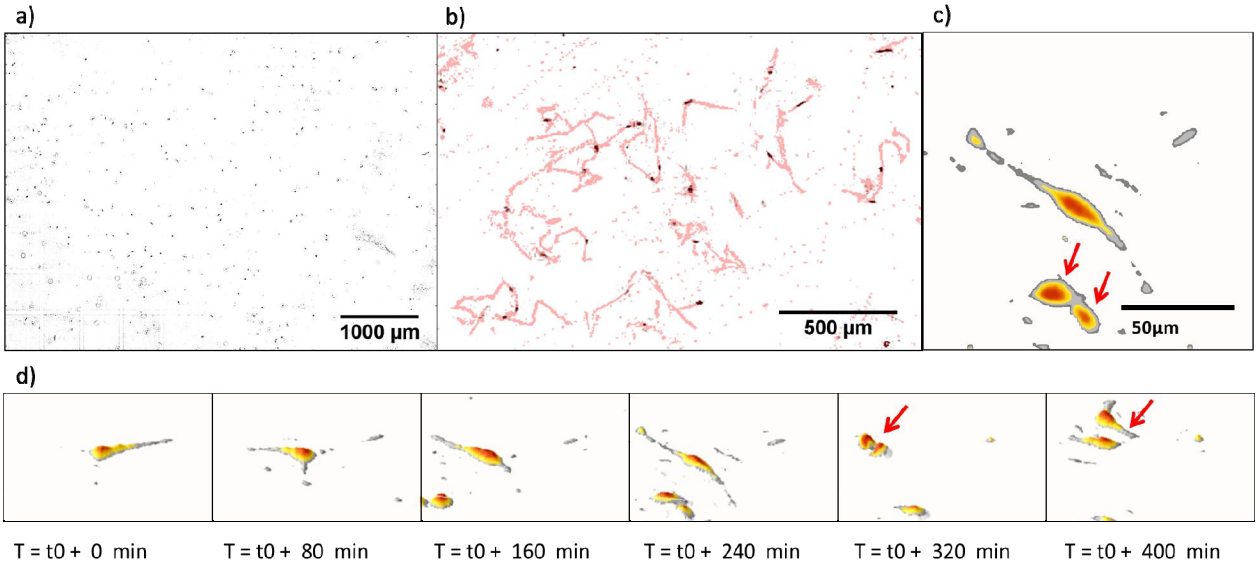

Figure 2. After holographic reconstruction the video lensfree microscopy device offers a resolution close to 2 µm over a field of view of 24 mm². (a) Reconstructed image showing cells in a field of view of 24 mm². (b) Trajectories in red followed by cells (black dots) during 7 hours of imaging inside the incubator. (c) Reconstructed image of a moving cell (filopodial extensions) and a dividing cell (red arrows). The grey/yellow/red lookup table reflects the reconstructed amplitude. (d) 3D reconstruction montage of a moving cell which later divides (red arrow). Cell thickness is obtained from the phase reconstruction.

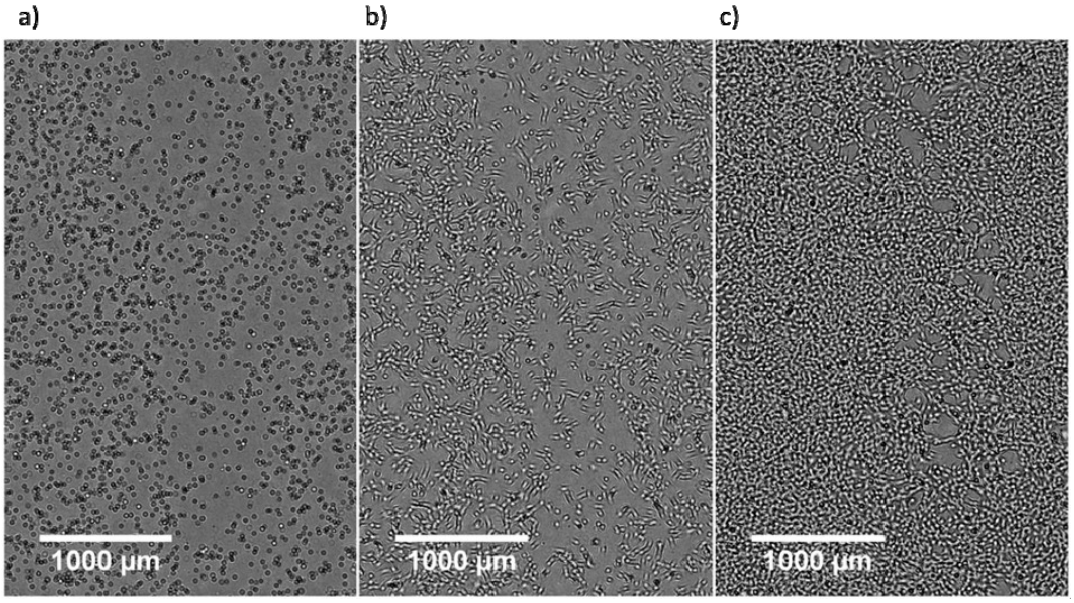

Figure 3. Video lensfree microscopy allows catching the three main steps of the cell culture of NIH 3T3 fibroblasts, *i.e.*, cell seeding, cell proliferation and confluence. NIH 3T3 fibroblast cells were grown in Dulbecco's Modified Eagle's Medium (DMEM). The above pictures are cropped regions of the larger 24 mm^2 acquisitions. After cell adhesion (a), cell spreading is later followed by cell population growth (b). This stage lasts for a few days until confluence is reached (c). During the proliferation phase many single events are recorded by lensfree imaging, *e.g.*, cell division, cell differentiation, morphogenesis, movement, detachment, *etc.*

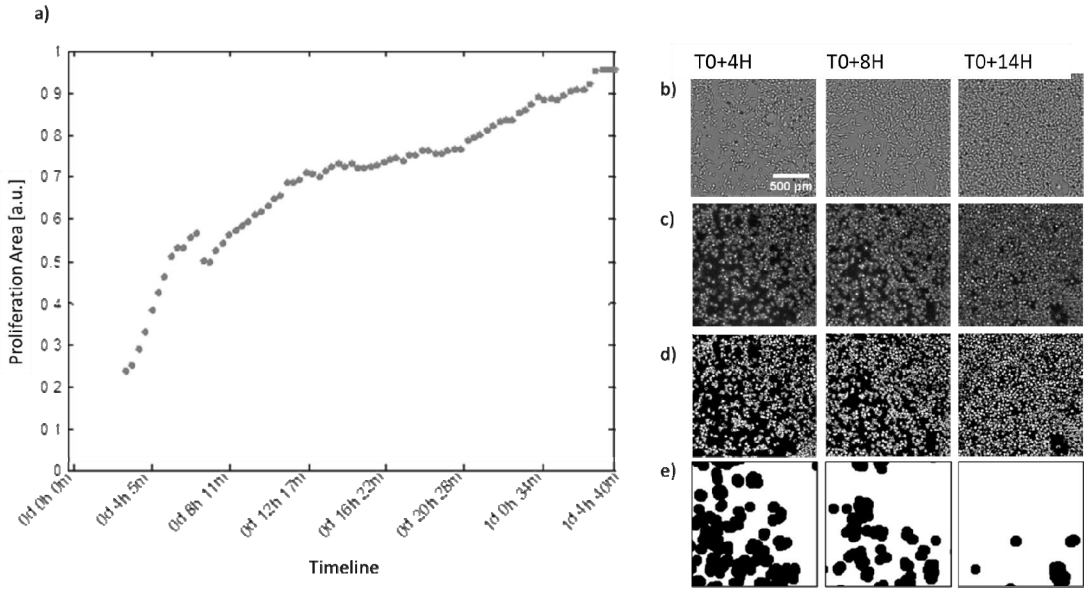

Figure 4. The measure of the confluence of NIH 3T3 fibroblast cells (a) is obtained as a first approximation by segmenting the textures in the raw lensfree acquisitions (b). The gradient image is calculated by applying a Sobel filtering (c). The area involving the higher variance in the gradient corresponds to the textured area, while the background's gradient remains flat. The gradient image is automatically thresholded using a Kmeans algorithm detecting two classes. Binary images locating the maxima of the gradient, delimiting the texturized features in the images, are obtained (d). A morphological closure of the obtained binary images allows filling the holes of the identified area corresponding to the low gradient which has not been attributed to the cells' class (e). Counting the ratio of white pixels over the whole pixels in the resulting segmented images allows calculating the relative amount of proliferation (a). The discontinuity at ~6 h is due to cell culture medium replacement which has slightly shifted the Petri dish.

At first, we will describe a regular cell culture experiment which serves as control in most bio-assays. A standard cell culture experiment can be divided in three successive steps, *i.e.*, cell seeding, cell proliferation and full confluency. Overall cell proliferation lasts few days depending on the initial cell density and proliferation rate. A time-lapse series corresponding to the three proliferation steps of a cell culture can be monitored from cell seeding to confluence (Fig. 3). The magnified regions of interest show the increase in cell density over time. In order to estimate the confluency, *i.e.*, the percentage of the surface covered by the cell culture, the raw acquisitions were segmented without the use of holographic reconstruction. The plot of the confluency as a function of time is given in Fig. 4 for a culture of NIH 3T3 fibroblast cells. The calculation is overestimated since the surface covered by the holographic patterns is larger than the true surface covered by the cells. Yet this method gives a relative amount of confluency which is sufficient to perform monitoring or comparative measurements between different experiments. Truly quantitative measurement of the proliferation rate can be performed by further looking at the single cell level and counting for every single cell division. We have shown in a previous paper [19] that cell detachment during division can be detected and used to measure the proliferation rate in a straightforward manner.

In addition, video lensfree microscopy distinguishes among different cell lines when observing both at mesoscopic and single cell levels. Fig. 5 shows acquisitions of different cell lines, respectively mesenchymal stem cells MSC, fibroblast cells NIH 3T3, prostate epithelial cells RWPE-1, keratinocyte cells HaCaT, umbilical vein endothelial cells HUVEC and osteosarcoma cells U2OS. The cell density, size and orientation can be visualized. Normal shape and agglomeration are observed for every cell line. Among the cell types, MSC stem cells, NIH 3T3 cells and U2OS cells (Fig. 5a,b,f) are well spread over the substrate with a low tendency to formation of clusters, yet cells are connected to each other. On the opposite, RWPE-1 cells and HaCaT cells are seen as clusters (Fig. 5c,d). Compared to RWPE-1 cells, the HaCaT cells are larger and tend to form a continuous monolayer of cells. On the other hand, the HUVEC cells stand out from the rest, forming a network between dense clusters of cells (Fig. 5e). When we add the ability to record movies and not only a static snapshot of a large portion of these cell populations we end up with a unique platform to study the spatial organization and its evolution over time. These observations allow describing a dynamic phenotype for the different cell lines at scales of different orders in magnitude ranging from micrometer to millimeter. To this respect the most striking example is the formation of networks observed with the cultures of HUVEC endothelial cells as shown in Fig. 6 and 7.

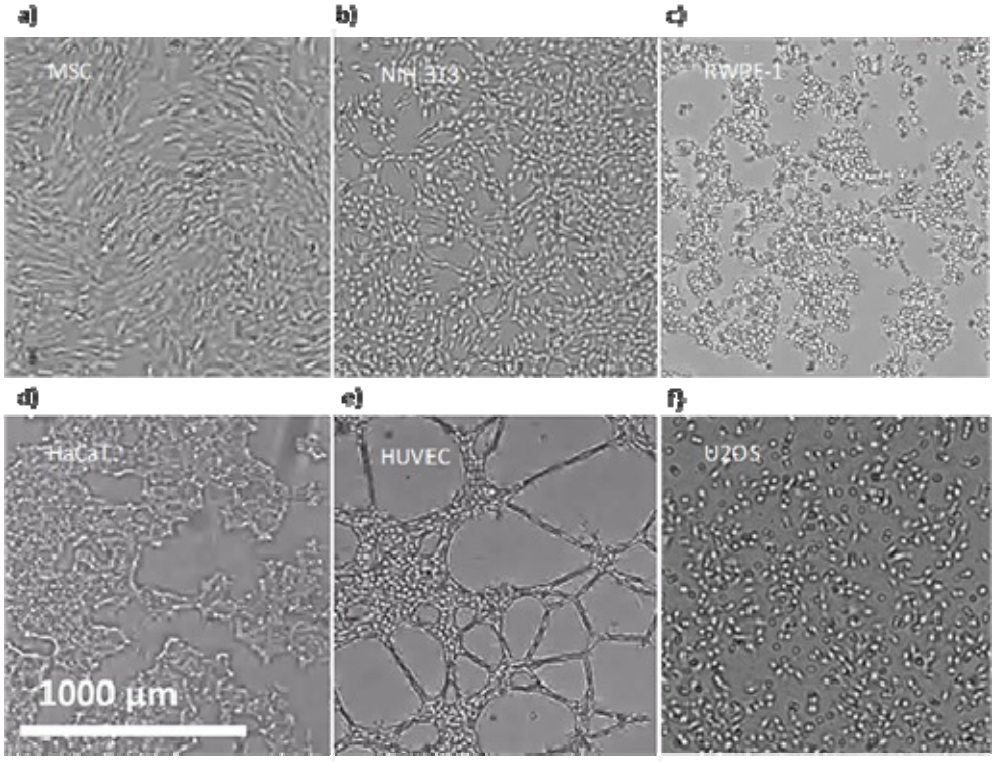

Figure 5. Visualization of various cell lines. (a) Mesenchymal stem cells MSC. (b) Fibroblast cells NIH 3T3. (c) Prostate epithelial cells RWPE-1. (d) Keratinocyte cells HaCaT. (e) Umbilical vein endothelial cells HUVEC. (f) Osteosarcoma cells U2OS. All cells were cultured at the bottom of a Petri dish, except HUVEC cells which were seeded on Matrigel (BD Biosciences).

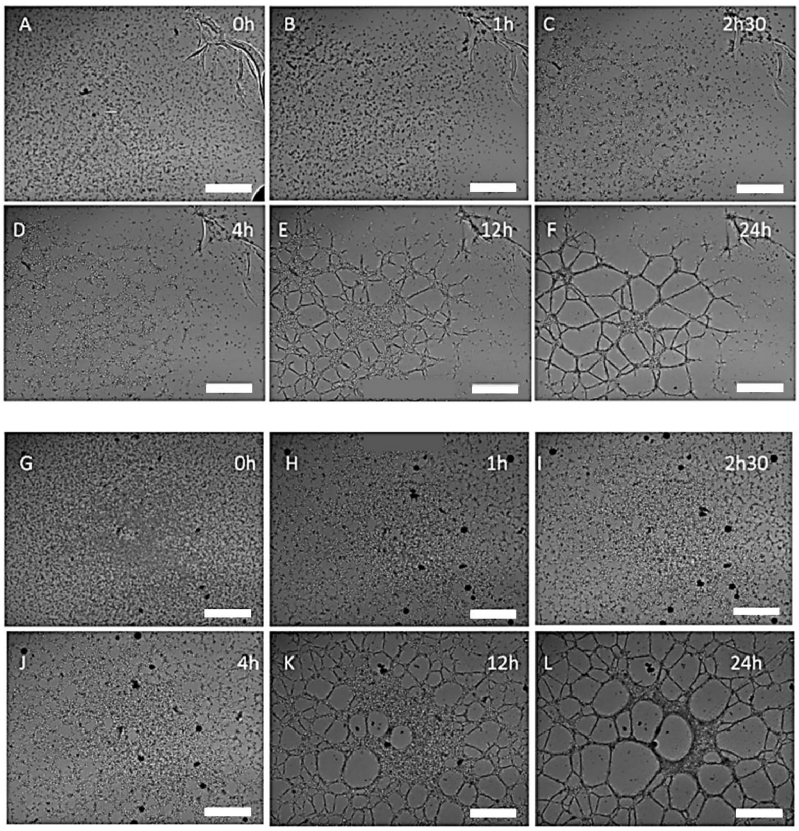

Figure 6. Network formation with HUVEC cells observed by means of lensfree video microscopy over 24 h. (A-F) and (G-L) are two distinct experiments. In the center of Petri dishes, a hole of 1 cm in diameter was drilled and sealed at the bottom with a quartz lamella. 75 µl of liquid Matrigel at 5 °C was added in the drilled hole and allowed to solidify in an incubator at 37 °C for 20 minutes. 5.10^4 HUVEC cells were then seeded on Matrigel (BD Biosciences) and incubated at 37°C. Scale bar is 1 mm.

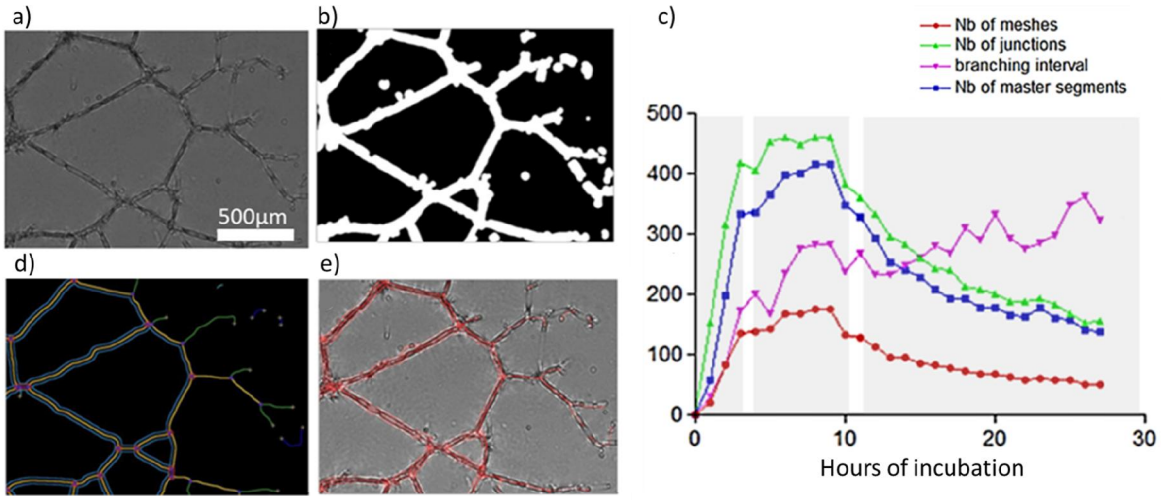

Figure 7. Steps of image processing of a HUVEC network. (a) Crop from the original image. (b) Image after binarization. (d) Image after the application of an angiogenesis analyzer algorithm. Segments are in yellow, branches in green, red points are nodes, meshes (closed structures, also called tube-like-structures) are in cyan, and isolated structures are in blue. (e) Merge of (a) and (d) for comparison. (c) Analysis of a HUVEC network as a function of incubation time in terms of number of meshes (red), junctions (green), branching interval (purple) and master segments (blue). Three successive steps are observed (dashed grey in (c)), *i.e.*, an initiation phase, a stabilization period and then the fusion of meshes.

The HUVEC network is a classical and well known phenomenon [20,21] and lensfree imaging is an innovation to study it. Formation of the network over a period of 24 hours is monitored in time-lapse mode (Fig. 6). The architecture of the HUVEC network was analyzed with ImageJ using an angiogenesis analyzer plug-in [22] to calculate several parameters of the network, including the number of branches, nodes and meshes, and then plot them as a function of time (Fig. 7). During the first 4 hours, the network is in formation: the number of meshes is increasing, so do the number of segments, junctions and nodes. Then, for 6 hours, the network is stable. In the end, the meshes merge to form larger meshes. After 24 h, the networks present the following architecture: total meshes area is around 9 mm², the number of meshes is approximately 60, and their mean size is 0.15 mm². Overall, we were able to define three different steps for the network formation: initiation, a stabilization period and then the fusion of meshes (Fig. 7c).

Although most of the fundamental biology experiments and research are performed with 2D cell culture models, 3D cell culture is a growing field aimed at mimicking the functions of living tissues present in the body. Essential cellular functions that are present in tissues are missed by adherent cell cultures [23]. However, monitoring a 3D cell culture in real time is a challenging task. Electric cell-substrate impedance sensing may not be effective to characterize a 3D cell culture as the cell aggregates do not attach to the substrate as firmly as in 2D cell culture environment, and conventional video microscopy techniques is challenged by the constant loss of focus that may result from the movement of the cells in the Z-plane and focus drift of the microscope. However, lensfree video microscopy is immune to the limitations caused by the constant loss of focus, since the setup is devoid of magnification lenses. Hence lensfree video microscopy is one of the very few techniques that can efficiently monitor 3D cell cultures in real time. Here, we demonstrate the real-time cell culture monitoring of RWPE-1 cells using lensfree video microscopy. Different holographic patterns of RWPE-1 cells in 2D and 3D cell cultures are obtained using lensfree video microscopy (Fig. 8). In 3-dimensional Matrigel culture, RWPE-1 cells organize into acini, *i.e.*, 3D clusters of cells that resemble to many-lobed berries. In previous work we have shown that the obtained holographic signature of RWPE-1 aggregates allows discriminating acini with lumen from spheroids which are tumoral like [24]. Spatial organization of RWPE-1 cells in a 3D volume was studied over time. Fig. 9 shows the development of an acinus over 72 hours. An initial stage, where the acinus grows up fast to a diameter of approximately 50 µm in 6 hours, can be distinguished. Further, the acinus grows up to approximately 100 µm in diameter in a long period of 42 hours. Finally the dimensions of the acinus remain stable during the next 24 hours. These results pave the way of future studies in the realms of fundamental biology that would not be envisaged by means of a 2D cell culture.

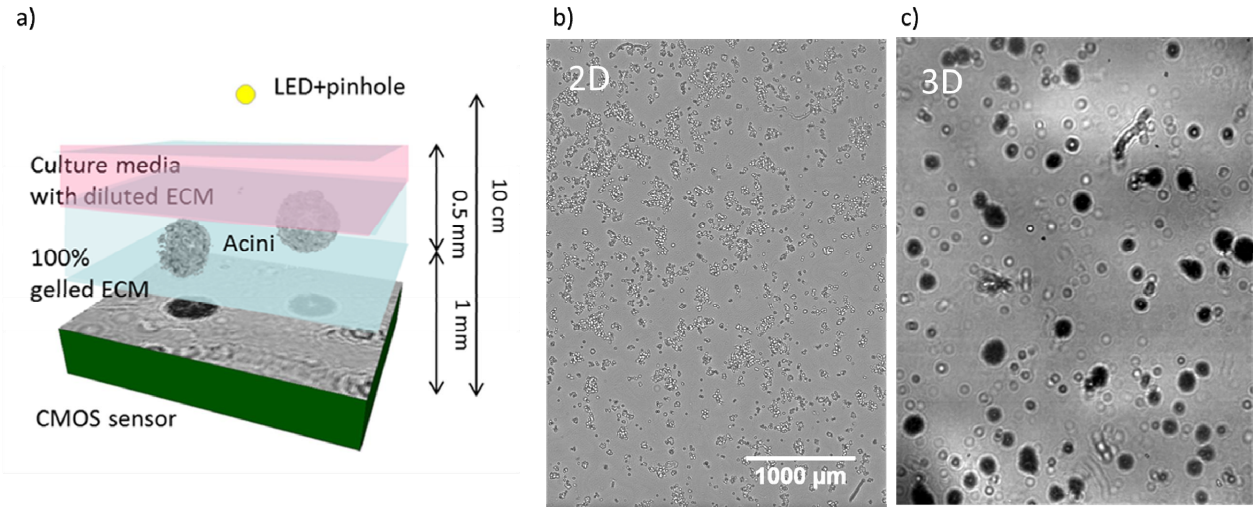

Figure 8. (a) Schematic of the lensfree imaging setup for 3D cultures of epithelial cells (not to scale). Epithelial cells are completely embedded within the extracellular matrix (ECM). (b) RWPE-1 adherent cells cultured at the bottom of a Petri dish and (c) cultured in a 3D extracellular matrix. The acini are clearly seen in (c) as large dark patterns. These are 3D polarized structures of cells and of 100 µm in diameter.

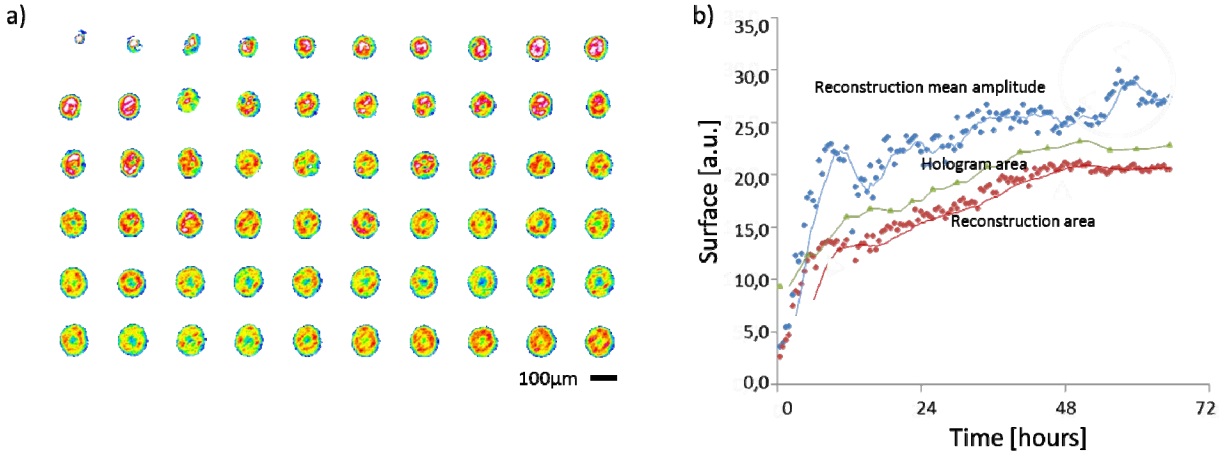

Figure 9. (a) Time-lapse observations showing the development of a prostatic acinus over 72 hours, with 1 hour between two frames. The reconstructed amplitude indicated as a grey/yellow/red lookup table allows to outline the acinus, but the value is likely incorrect and is given for information only. (b) The relative dimensions of the acinus is measured over time by means of three different metrics, *i.e.*, the raw hologram area (green curve), the mean amplitude of the holographic reconstruction (blue curve) and at best by the surface of the reconstructed amplitude (red curve). The latter parameter gives the dimension of the 2D projection of the acinus figure and can be related to the diameter of the 3D volume of the acinus provided that it is spherical.

4. CONCLUSION

We have reported lensfree video microscopy as a tool to monitor cell cultures in an incubator over periods of time ranging from a few minutes to several weeks. Versatility of video lensfree imaging was demonstrated by observing various cell types in both 2D and 3D cell culture environments. Lensfree video microscopy can facilitate high throughput label-free cell assays in the fields of fundamental research, tissue regeneration, drug development and toxicology studies by offering a large field of view and simplicity. The system offers a resolution close to 2 µm over a field of view of 24 mm², which makes it capable of monitoring a cell culture at different scales, from a very large field of view down to the single cell. In combination with 3D cell culture, it allows to probe models that mimic functions of living tissues.

REFERENCES

[1] Zhao, L., Lee, V. K., Yoo, S. S., Dai, G. & Intes, X. "The integration of 3-D cell printing and mesoscopic fluorescence molecular tomography of vascular constructs within thick hydrogel scaffolds. Biomaterials," 33, 5325–5332. (2012).
[2] Jiang, Y., Tong, Y. & Lu, S. "Visualizing the three-dimensional mesoscopic structure of dermal tissues." J. Tissue Eng. Regen. Med., doi: 10.1002/term.1579. (2012).
[3] Bian, W., Liau, B., Badie, N. & Bursac, N "Mesoscopic hydrogel molding to control the 3D geometry of bioartificial muscle tissues." Nat. Protocol., 4, 1522–1534. (2009).
[4] Kalay, Z. "Fundamental and functional aspects of mesoscopic architectures with examples in physics, cell biology, and chemistry." Crit. Rev. Biochem. Mol. Biol., 46(4), 310-326. (2011).
[5] Gabor, D. "A new microscopic principle. Nature," 161, 777-778. (1948).
[6] Repetto, L., Piano, E., Pontiggia, C. "Lensless digital holographic microscope with light-emitting diode illumination. » Opt. Lett., 29(10), 1132-1134. (2004).
[7] Su, T. W., Seo, S., Erlinger, A. & Ozcan, A. « High-throughput lensfree imaging and characterization of a heterogeneous cell solution on a chip." Biotechnol. Bioeng., 102(3), 856-868. (2009).
[8] Isikman, S. O., Bishara, W., Mavandadi, S., Yu, F. W., Feng, S., Lau, R. & Ozcan, A. "Lens-free optical tomographic microscope with a large imaging volume on a chip." Proc. Natl. Acad. Sci. U.S.A., 108(18), 7296–301. (2011).

[9] Isikman, S. O., Greenbaum, A., Luo, W., Coskun, A. F. & Ozcan, A. "Giga-pixel lensfree holographic microscopy and tomography using color image sensors." PLoS ONE, 7(9), e45044. (2012).
[10] Greenbaum, A., Luo, W., Su, T. W., Göröcs, Z., Xue, L., Isikman, S. O. *et al.* "Imaging without lenses: achievements and remaining challenges of wide-field on-chip microscopy." Nat. Methods, 9(9), 889-895. (2012).
[11] Zheng, G., Lee, S. A., Antebi, Y., Elowitz, M. B. & Yang, C. "The ePetri dish, an on-chip cell imaging platform based on subpixel perspective sweeping microscopy (SPSM)." Proc. Natl. Acad. Sci. U.S.A., 108(41), 16889-16894. (2011).
[12] Han, C., Pang, S., Bower, D. V., Yiu, P. & Yang, C. "Wide field-of-view on-chip Talbot fluorescence microscopy for longitudinal cell culture monitoring from within the incubator." Anal. Chem., 85(4), 2356-2360. (2013).
[13] Jin, G., Yoo, I. H., Pack, S. P., Yang, J. W., Ha, U. H., Paek, S. H. & Seo, S. "Lens-free shadow image based high-throughput continuous cell monitoring technique. Biosens. Bioelectron,". 38(1), 126-131. (2012).
[14] Flaccavento, G., Lempitsky, V., Pope, I., Barber, P. R., Zisserman, A., Noble, J. A. & Vojnovic, B. "Learning to Count Cells: applications to lens-free imaging of large fields." Microscopic Image Analysis with Applications in Biology, (2011).
[15] Fienup, J.R. "Phase retrieval algorithms: a comparison." Appl. Opt., 21(15), 2758–69. (1982).
[16] Denis, L., Fournier, C., Fournel, T. & Ducottet, C. "Twin-image noise reduction by phase retrieval in in-line digital holography." Optics & Photonics 2005, p. 59140J. (2005).
[17] Coskun, A. F., Sencan, I., Su, T. W. & Ozcan, A. "Lensless wide-field fluorescent imaging on a chip using compressive decoding of sparse objects." Opt. Express, 18(10), 10510-10523. (2010).
[18] Greenbaum, A., Luo, W., Khademhosseinieh, B., Su, T. W., Coskun, A. F. & Ozcan, A. "Increased space-bandwidth product in pixel super-resolved lensfree on-chip microscopy." Sci. Rep., 3, 1717. (2013).
[19] Kesavan, S. V., Allier, C. P., Navarro, F., Mittler, F., Chalmond, B. & Dinten, J.-M. "Lensless imaging system to quantify cell proliferation." SPIE BiOS, p. 858708. (2013).
[20] Serini, G., Ambrosi, D., Giraudo, E., Gamba, A., Preziosi, L. & Bussolino, F. "Modeling the early stages of vascular network assembly." EMBO J., 22(8), 1771-1779. (2003).
[21] Montesano, R., Orci, L. & Vassalli, P. "In vitro rapid organization of endothelial cells into capillary-like networks is promoted by collagen matrices." J. Cell Biol., 97(5), 1648-1652. (1983).
[22] Carpentier G., Angiogenesis Analyzer plugin for ImageJ available online at: http://imagej.nih.gov/ij/macros/toolsets/angiogenesis analyzer.txt.
[23] Pampaloni, F., Reynaud, E. G. & Stelzer, E. H. "The third dimension bridges the gap between cell culture and live tissue." Nat. Rev. Mol. Cell Biol., 8(10), 839-845. (2007).
[24] Dolega, M. E., Allier, C., Vinjimore Kesavan, S., Gerbaud, S., Kermarrec, F., Marcoux, P., Dinten J.-M., Gidrol. X. & Picollet-D'hahan, N. "Label-free analysis of prostate acini-like 3D structures by lensfree imaging." Biosens. Bioelectron., 49, 179-183. (2013).